Deformation of Poly(dimethylsiloxane) Oligomers under Uniaxial Tension: Quantum Chemical View

E. A. Nikitina

Institute of Applied Mechanics, Russian Academy of Sciences, Leninsky prospekt, 31A, Moscow, 117334 Russia

V. D. Khavryutchenko

Institute of Surface Chemistry, National Academy of Sciences of Ukraine, Kiev, 252028 Ukraine

E. F. Sheka*

Russian Peoples' Friendship University, General Physics Department, ul.Ordjonikidze, 3, Moscow, 117923 Russia

H. Barthel and J. Weis

*Wacker-Chemie GmbH, Werk Burghausen, D-84480 Burghausen, Germany*

The response of a silicone polymer fragment to external stresses is considered in terms of a mechanochemical reaction. The quantum chemical realization of the approach is based on a coordinate-of-reaction concept for the purpose of introducing a mechanochemical internal coordinate (MIC) that specifies a deformational mode. The related force of response is calculated as the energy gradient along the MIC, while the atomic configuration is optimized over all of the other coordinates under the MIC constant-pitch elongation. The approach is applied to a set of linear silicone oligomers Si_n with $n = 4$, 5, and 10 subjected to uniaxial tension, followed by the molecule breaking and a postfracture relaxation. Three stages of deformation, differing by structural transformation, have been detected. The observed peculiarities of the oligomer mechanical behavior are well attributed to the characteristic modes of vibrational spectra. The oligomer strength and the related Young's moduli are obtained. A cooperative radical-driven mechanism of silicone polymer fracture is suggested.

Introduction

Silicone elastomers span a large field of experimental studies and technical applications,[1] while microscopic attempts to examine their mechanical properties are not known. Thus, the reasons for the high elasticity of the polymers are discussed only qualitatively. The quantitative foundations for the chemical bond scission as well as for the bulk body fracture are fully obscure. At the same time, a theoretical study of the polymer behavior under external stress is quite developed. Two approaches are known to describe the mechanical properties of the bodies quantitatively. The first one, which might be called a *dynamical approach*, is based on the calculation of the energy of elastic deformation of a polymer by evaluating the related force constants of the body in either a classical physical[2] or a quantum chemical (QCh)[3,4] manner. The approach is mainly aimed at the determination of elastic constants such as Young's moduli. In the classical physical manner, it has received a wide recognition as applied to organic polymers (see ref 2 and references therein). The other *atomically microscopic approach* was proposed in the early 1970s[5] and was aimed at a QCh consideration of a chemical bond breaking. In this paper, two seven-member oligomers of polyethylene with different peripheral chemical groups subjected to uniaxial tension were considered. It was the first time that a stress−strain interrelation had been obtained quantum chemically. Since then, two other attempts in the QCh manner of such interrelation have been

made with respect to an ethane molecule[6] and a solitary Si−O bond.[7] Despite a clearly seen restriction of the first, these results clearly suggest a doubtless advantage of the QCh approach to the treatment of the mechanical phenomena. Active development of quantum chemical tools as well as a steady build-up of computer facilities have made it possible to come back to the problem and to raise the question about a transformation of modern computational chemistry into *computational mechanochemistry*. General concepts of such a transformation have been considered in ref 8. These concepts applied to the description of the deformation of a heptane molecule, a fragment of propylene polymer, and a piece of bulk silica were quite successful and informative.[8]

In this paper, the suggested quantum mechanochemical (QMCh) approach is applied to three linear poly(dimethylsiloxane) (PDMS) oligomers Si_n described by the general formula

$$(CH_3)_3\, SiO\text{-}[(CH_3)_2SiO]_{n-2}\text{-}Si(CH_3)_3$$
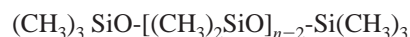
with $n = 4$, 5, and 10, subjected to uniaxial tension. An extended computational experiment has been carried out by using the QMCh software DYQUAMECH[9] that exploits one of the high-level semiempirical techniques (PM3 in the current study). The choice of uniaxial tension is not crucial for the approach suggested, and the preference toward this deformational mode was only due to its wide application in practice. As was shown, the approach highlights well the mechanochemical reactions of

the siloxane chain breaking and unambiguously discloses their character (homo- or heterolytical) with respect to the reaction products. It provides a researcher with energy−strain, force−strain, and stress−strain interrelations and conveys the reasons for high elasticity and elastic behavior of the oligomer as well as for the stress−strain hysteresis. It also makes an allowance for the determination of the oligomer strength, Young's modulus, and the work of deformation needed for the bond scission. In comparing calculated and experimental data, a cooperative radical-driven reaction of a chemical bond breaking was suggested to be responsible for the bulk silicone polymer fracture, an extension of a concept widely known for organic polymeric substances.[2,10]

The paper is organized as follows. Section 1 describes the grounds for the quantum mechanochemistry. Atomic reconstruction at all stages of the deformation of the oligomers subjected to uniaxial tension is considered in section 2. Products of the mechanochemical reactions are discussed in section 3. Dynamical characteristics of the oligomers studied are presented in section 4. Young's moduli are discussed in section 5. Section 6 concerns the mechanism of the PDMS polymer fracture. The conclusion summarizes the essentials obtained during the study.

Quantum Mechanochemical Approach

Grounds for the QMCh approach, suggested by authors, are described elsewhere.[8] The approach states that a fracture is a *mechanochemical reaction* proceeding in a loaded body and resulting in an interatomic bond rupture (scission).[11−17] A similarity between mechanically induced reaction and the first-type chemical ones, first pointed out by Tobolski and Eyring 50 years ago,[18] suggested the use of a well developed QCh approach of the reaction coordinate[19] in the study of atomic structure transformation under deformation. The main point, therewith, concerns the coordinate defining. When dealing with chemical reactions, a reaction coordinate is usually selected among the internal ones (valence bond, bond angle, or torsion angle) or a linear combination of them. Similarly, *mechanochemical internal coordinates* (MICs) were introduced[8] as modified internal coordinates defined in such a way as to be able to specify the considered deformational modes. The MICs were thus designed to meet the following requirements.

(1) Every MIC is a classifying mark of a deformational mode.

(2) Every MIC is determined in much the same way as the other internal coordinates except for a set of specifically selected support atoms.

(3) The MIC relevant to a particular deformational mode is excluded from the QCh optimization procedure when seeking the minimum of the total energy.

(4) A *response force* is determined as the residual gradient of the total energy along the selected MIC.

If experimentally the structure deformation is a response of the application of external forces, computations so far have been logically inverted; they were aimed at the evaluation of response forces (forces of resist[6,7]), while the corresponding MIC changes in a constant-pitch manner. This logic is dictated by the general architecture of the conventional QCh software where the force calculation, namely, the total energy gradient calculation, is the key procedure.

The QMCh software DYQUAMECH is based on the QCh software DYQUAMOD[20] which exploits advanced semiempirical QCh methods (MNDO, MNDO/H, AM1, and PM3) and is very efficient for large clusters calculations (see review[21]). Three important innovations were added to the main body of DYQUA-

MOD to create DYQUAMECH: (i) the MIC input algorithm; (ii) the computation of the total energy gradients both in the Cartesian and internal coordinates; (iii) the optimization performance in the internal coordinates.

MIC Input Algorithm. Every MIC is determined by a set of support atom groups. Each group can contain either one support atom or a few ones depending on which atoms participate in the mechanical support of the cluster. If a group is the case, a synchronism in the support atom behavior should be provided. Formally, this is achieved by inputting support atoms specifically listed. The MIC type determines the number of the lists; two lists are needed for uniaxial deformational mode, three lists for a bending mode, and four lists for a twisting mode. The first atoms in the lists always determine the MIC itself. Besides the atoms belonging to the cluster, the lists contain some fictitious auxiliary atoms which assist in a redetermination of the support atom coordinates. The latter is aimed at the creation of identical orthogonal systems of internal coordinates related to every atom from the list. One of these coordinates becomes a MIC with respect to the deformational mode considered. The others are optimized fully independently from the MIC because the forces aligned along them have no projections on the MIC.

Force Calculations. The forces, which are the first derivatives of the electron energy $E(R)$ with respect to the atom coordinates R in Cartesian coordinates, can be determined analytically according to the expression[22]

$$\frac{dE}{dR} = \left\langle \phi \left| \frac{\partial H}{\partial R} \right| \phi \right\rangle + 2\left\langle \frac{\partial \phi}{\partial R} \left| H \right| \phi \right\rangle + 2\left\langle \frac{\partial \phi}{\partial P} \left| H \right| \phi \right\rangle \frac{dP}{dR} \qquad (1)$$

Here, ϕ is the electron wave function of the ground state at fixed nucleus positions, H represents the adiabatic electron Hamiltonian, and P is the nucleus pulse. When calculating (1), a quite efficient computational technique suggested by Pulay[23] was applied. When the force calculations are complete, the gradients are redetermined in the system of internal coordinates in order to proceed further in seeking the total energy minimum by atomic structure optimization.

Optimization in Internal Coordinates. As is well-known (see, for instance, ref 24), the structure optimization performed in the internal coordinates requires much less time due to better coordinate separation. As a consequence of the coordinate transformation, the energy gradients are determined as follows:

$$\frac{\partial E}{\partial Q_k} = \sum_{i=1}^{3N} \frac{\partial E}{\partial R_i} \frac{\partial R_i}{\partial Q_k} \qquad (2)$$

where N is the number of atoms, while R_i and Q_k are the ith Cartesian and the kth internal coordinates, respectively; the latter involve a considered MIC as well. The calculation of $\partial R_i/\partial Q_k$ is carried out by a conventional five-point formula that reduces the computational time approximately by an order of magnitude and permits performing the calculations for large cluster systems on high-speed personal computers.[20] The following characteristics are thus obtained when a computational cycle is completed.

(1) The atomic structure of the loaded body at any stage of the deformation including bond scission and post-breaking relaxation. Post-breaking fragments can be easily analyzed therewith by just specifying them as the products of either homolytic or heterolytic reaction.

(2) A complete set of dynamical characteristics of the deformation performed which are expressed in terms of energy−elongation, force−elongation, and stress−strain interrelations.

Deformation of Poly(dimethylsiloxane) Oligomers
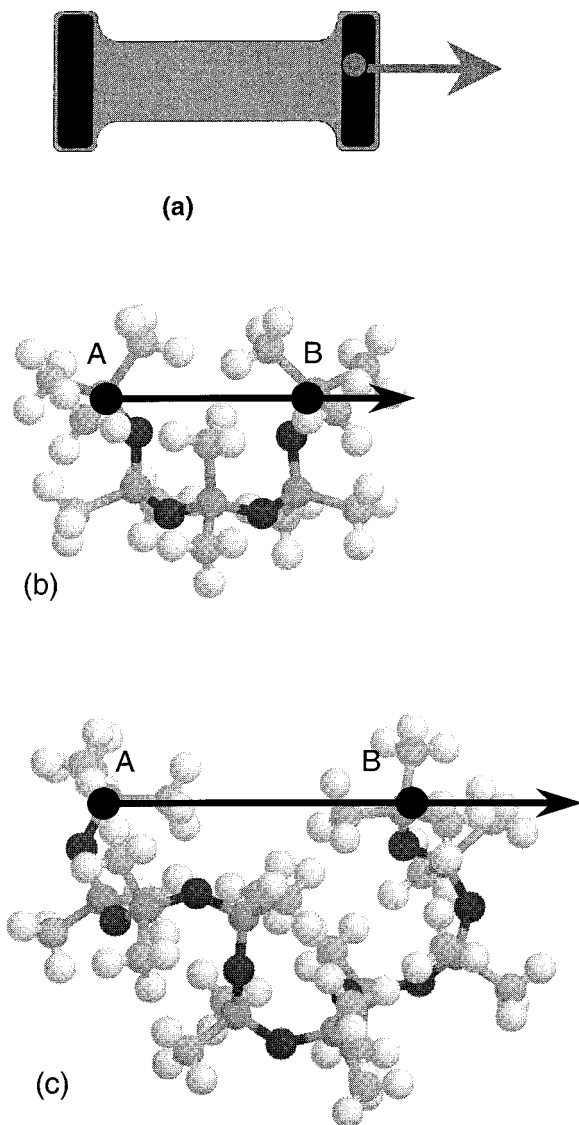
J. Phys. Chem. A, Vol. 103, No. 51, 1999 **11357**

Figure 1. Scheme of uniaxial tensile loading. (a) A standard scheme of loading at uniaxial deformation. (c and b) Definition of the uniaxial tensile MIC for the Si5 and Si10 oligomer molecules, respectively,

Analysis of the relevant curves highlights the mechanical behavior of the loaded body at all stages of the deformation considered.

(3) Mechanical characteristics of the body determining its strength (the maximal stress value); the work needed for the deformation performed, including chemical bond scission; and the Young's modulus describing the body behavior in the elastic deformation regime.

4. Vibrational spectrum of the body at any stage of the deformation.

In what follows, the first three above-listed topics will be presented with respect to three silicone oligomers. The calculations were performed on a two-processor PentiumPro PC.

Response of Atomic Configuration to Uniaxial Tension

Figure 1 shows a scheme of loading examined in the study. According to a conventional experimental setup where one end of the loaded body is fixed and the other is loaded by a weight, the uniaxial-tension MIC selected for the QMCh study connects a fixed end of the oligomer molecule (A) with a moving one (B). The MIC elongation proceeds in a pitch-constant way with the pitch value of 0.3 Å. A full optimization of the atomic

structure of oligomer molecules is carried out at each step of the elongation excluding the MIC only.

Figures 2 and 3 present sets of successive steps for the deformation of the Si5 and Si10 oligomers from the starting unloaded structure until the relaxed one when one of the Si−O bonds of the backbone siloxane chain is broken. As is clearly seen from the figures, in both cases the deformation proceeds as a three-stage process where the stages can be conditionally attributed to *torsion-angle* (stage 1), *bond-angle* (stage 2), and *valence-bond* (stage 3) *deformations*, respectively. The former deformation occurs when the MIC is lengthened from 6 to 9 Å for the Si5 molecule and from 6 to 12 Å for the Si10 one. It causes mainly a reorientation of methyl units with respect to the backbone siloxane chain followed by a minor changing in the bond angles O−Si−O and Si−O−Si. The bond angle deformation (the MIC length is in the regions of 9−12 Å and 12−20 Å for the Si5 and Si10 oligomers, respectively) concerns changes in the backbone bond angles Si−O−Si. As was said above, the calculations were performed using the PM3 QCh technique, which usually simulates the equilibrated value of the angle in the range 130−150°.[25] The tensile deformation stimulates an increase of the angle up to 180° that causes a vividly seen straightening of the siloxane chains of both molecules. Then starts the third stage, involving the stretching of valence bonds. This is well illustrated by Figure 4, which shows the change in the lengths of the Si5 (and/or Si10) molecule Si−O bonds under the deformation. Actually, in the deformation regions, allocated to stages 1 and 2, the bonds remain practically unchanged. However, when the MIC length reaches 12 Å, a clearly seen quasilinear elongation of all bonds occurs. The bonds behave quite similarly, therewith. When the MIC length comes up to 15 Å, the breaking of bond 8 takes place. Afterward, bond 7 shortens noticeably while other bonds approach the equilibrated value.

Since every mechanical deformation is thought to be vibration-involving,[2] the suggested division should have a direct resemblance to the relevant vibrational spectrum of the molecule. Figure 5 presents the distribution of squared frequencies of vibrations related to the siloxane chain of the Si5 molecule, which defines the distribution of the related force constants[26] to a great extent. As seen from the figure, in full accordance with the above classification, the weakest bending vibrations of the Si−O−Si, O−Si−C, and C−Si−C angles and torsion vibrations are related to the methyl units which open the list and are followed by the bending vibrations of the O−Si−O type. The stretching vibrations of the Si-0 bonds complete the list. Because of the obvious resemblance between the energy scale succession of the main dynamic characteristics of the species and its mechanical behavior, a qualitative prediction of the latter can be suggested by analyzing the properly assigned vibrational spectrum.

As follows from Figure 4, all Si−O bonds behave quite similarly, excepting a particular one to be broken. This also follows from Figure 6 where the length change for every bond during the deformation at stage 3 is shown more obviously. Since the value of 1.65 Å, which is close to the equilibrated one, was taken as a reference point in Figure 6, the figure demonstrates the total elongation acquired by every bond during the deformation. As seen, all bonds are regularly strained in average, despite only the end bond 8 being loaded so that the total elongation of the MIC is distributed over all bonds uniformly enough. The bond break occurs when the relative elongation approaches 13%. Similar data are obtained for the Si10 oligomer as well. At the same time, the inner bonds 4 and
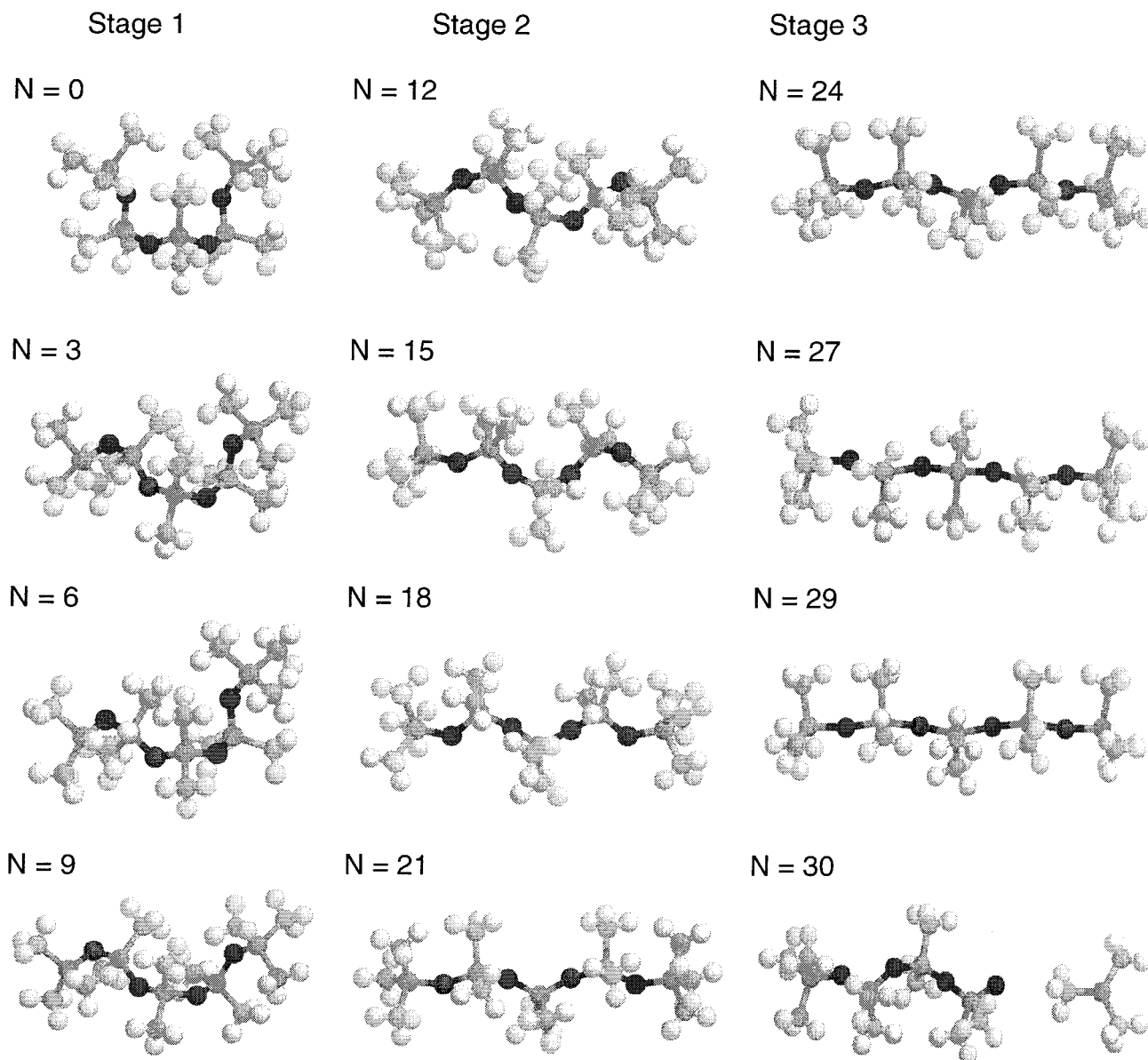
Stage 1   Stage 2   Stage 3

N = 0   N = 12   N = 24

N = 3   N = 15   N = 27

N = 6   N = 18   N = 29

N = 9   N = 21   N = 30

Figure 2. Successive steps of the Si5 molecule deformation. *N* numbers the steps with 0.3 Å pitch.
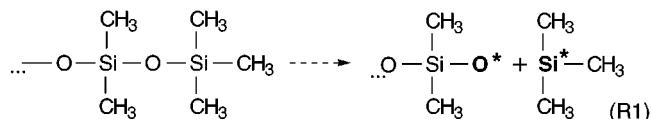
5, which are the most strained, are not broken, but the end bond 8, which is much less strained, is subjected to rupture.

To check whether a pitch value of 0.3 Å might cause the observed effect, calculations have been restarted at the step preceding the bond rupture with a lower pitch of 0.03 Å. The break of the same bond 8 has occurred after six steps. Again, restarting calculations immediately before the bond break with a still lower pitch of 0.003 Å, a rupture of bond 8 has been obtained after four steps. This means that some other reasons are responsible for the selection of the bond to be broken. Among the latter, one should take into account the heat of formation of the final products. Calculations have shown that the value is less by about 2 kcal/mol when final products correspond to the molecule division by a 1:4 silicon fraction instead of a 2:3 one.
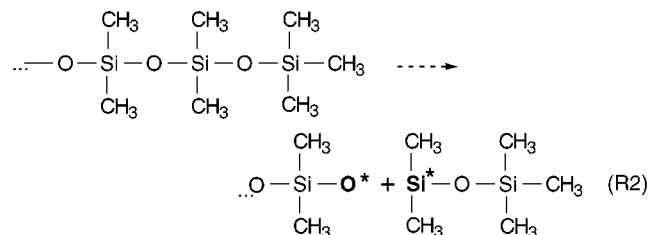
Products of the Mechanochemical Reaction

The reaction products formed when a Si—O bond is broken are shown in Figure 7. The case related to the loading scheme shown in Figure 1b is presented in Figure 7a. As seen from the figure, the reaction results in the formation of two stable noncharged fragments

$$...—O—\underset{\underset{CH_3}{|}}{\overset{\overset{CH_3}{|}}{Si}}—O—\underset{\underset{CH_3}{|}}{\overset{\overset{CH_3}{|}}{Si}}—CH_3 ----\rightarrow ..O—\underset{\underset{CH_3}{|}}{\overset{\overset{CH_3}{|}}{Si}}—O^* + \underset{\underset{CH_3}{|}}{\overset{\overset{CH_3}{|}}{Si^*}}—CH_3 \quad (R1)$$

To look if the result depends on the location of the bond subjected to breaking, a scheme of the Si5 molecule loading has been redesigned. The corresponding MIC connects the same fixed atom A as shown in Figure 1b but with another moving atom C (see insert in Figure 7). Under these conditions the inner bond 6 is broken (see Figure 7b). The breaking is followed by the formation of two intermediate noncharged fragments
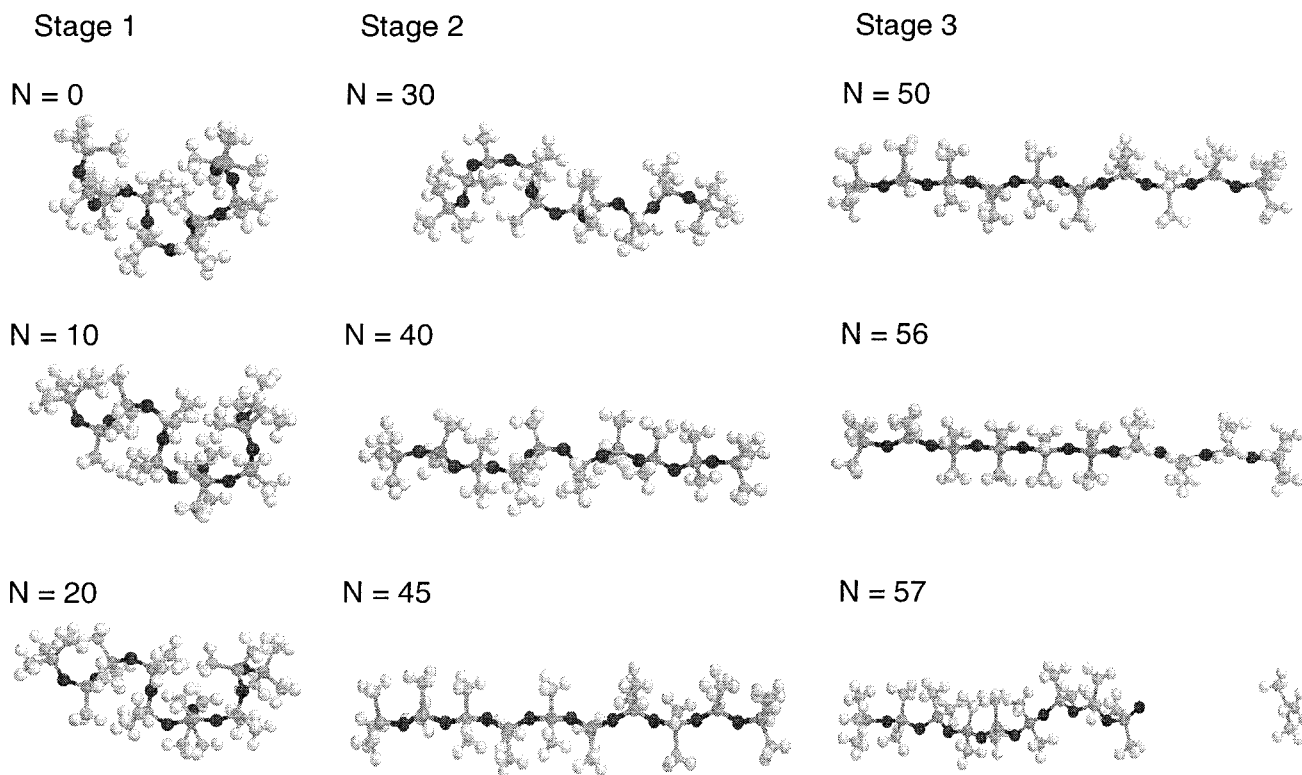
$$...—O—\underset{\underset{CH_3}{|}}{\overset{\overset{CH_3}{|}}{Si}}—O—\underset{\underset{CH_3}{|}}{\overset{\overset{CH_3}{|}}{Si}}—O—\underset{\underset{CH_3}{|}}{\overset{\overset{CH_3}{|}}{Si}}—CH_3 \quad ----\rightarrow$$

$$..O—\underset{\underset{CH_3}{|}}{\overset{\overset{CH_3}{|}}{Si}}—O^* + \underset{\underset{CH_3}{|}}{\overset{\overset{CH_3}{|}}{Si^*}}—O—\underset{\underset{CH_3}{|}}{\overset{\overset{CH_3}{|}}{Si}}—CH_3 \quad (R2)$$

Deformation of Poly(dimethylsiloxane) Oligomers

J. Phys. Chem. A, Vol. 103, No. 51, 1999 **11359**

Stage 1   Stage 2   Stage 3

N = 0   N = 30   N = 50

N = 10   N = 40   N = 56

N = 20   N = 45   N = 57

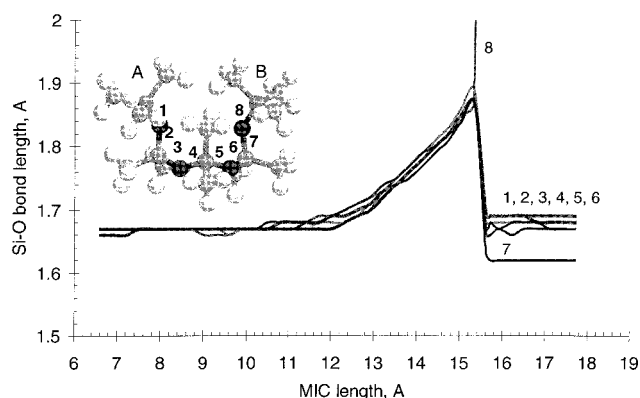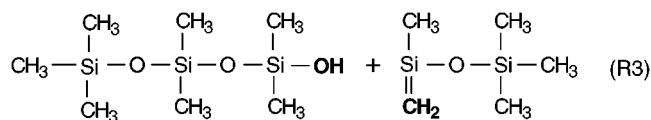**Figure 3.** Successive steps of the Si10 molecule deformation. N numbers the steps with 0.3 Å pitch.

Figure 4. Deformation of the Si−O bonds of the Si5 molecule under uniaxial tension. The bond numbering is given in the inserted molecular structure.

Figure 5. Density of the squared vibrational frequencies of the Si5 molecule.[26]

of head-end composition, which repeats those shown above and is completed by the formation of two stable molecules (see Figure 7c)

(R3)

Therefore, the broken chain ends are stabilized by the hydroxyl and methylene groups, respectively.

While the electronic properties of molecular fragments from (R3) are quite transparent, there is a need to find an adequate quantitative description of the scission fragments (R1) and (R2). A detailed consideration for the Si4 oligomer has been performed, and the relevant results are given in Table 1 for silicon and oxygen atoms of the molecular siloxane chain. The atom numbering corresponds to a successive position of the atoms in the chain. The results presented are easily generalized for all members of the Si_n oligomer family.
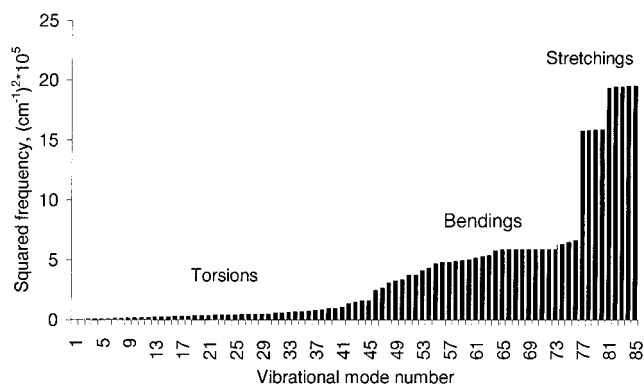
The data given in the table gives the following quantities. Column 3 presents the atomic charges expressed as

$$e_\nu = n_0 - (P^\alpha_{\nu\nu} + P^\beta_{\nu\nu}) \qquad (3)$$

Here, n_0 determines the number of the valence electrons of the atoms while $P^\alpha_{\nu\nu}$ and $P^\beta_{\nu\nu}$ correspond to the diagonal elements of the electron density matrices for α and β spins.[28] Atom spin density listed in column 4 is defined as the difference

$$\{Sp\}_\nu = P^\alpha_{\nu\nu} - P^\beta_{\nu\nu} \qquad (4)$$

The quantity characterizing a bonding between atoms μ and ν is described by the Wiberg's bond index (WBI)[29] expressed as

$$W_{\mu\nu} = (P^\alpha_{\mu\nu} + P^\beta_{\mu\nu})^2 \qquad (5)$$

The quantity is very useful to highlight atoms that are bonded to the given one. A sum of the WBIs over all atoms bonded to
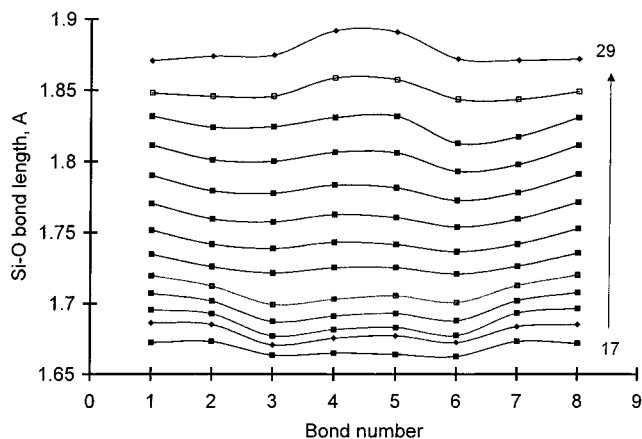
Figure 6. MIC elongation distributed over the Si−O backbone bonds of the Si5 molecule. The arrow indicates the growth of the step number.

the given one (data in column 5 of Table 1)

$$W_\nu = \sum_\mu W_{\mu\nu} \tag{6}$$

is of a particular interest in determining the number of valence electrons of the atom participating in the interatomic bonding thus describing its *coordination saturation*[30] or *effective valency*.[31] The upper limit of the latter approaches n_0, and its deviation from this value (see column 6 of Table 1), namely,

$$I_\nu = n_0 - W_\nu \tag{7}$$

if available, can be considered a latent valency or in accordance with[30] *an index of free valency* of the atom which highlights a potential chemical activity of the latter.

As seen from the table, the atomic characteristics of the unloaded Si4 molecule are as expected. The charge distribution over the atoms shows that there are two groups, each of two atoms, of positively charged silicon atoms. The charge value within each group is practically constant and differs by about 0.19 au for different groups. The finding is naturally explained by the related atom's surroundings. While inner atoms 3 and 5 are connected with two oxygen atoms and two methyl units each, the closest neighborhood of the end atoms 1 and 7 involves three methyl groups and a single oxygen atom. As for the oxygen atoms' charges, their values are practically constant along the siloxane chain. As must be expected, the atomic spin density is zero. The summary WBIs are close to 4 and to 2 for silicon and oxygen atoms, respectively, so that values of the free valency indices from column 6 are quite small. Quite similar results were obtained for the Si5 and Si10 oligomers in the closed-shell approximation.

When the molecule is broken, drastic changes occurred within the electronic characteristics of atoms 6 (**O**) and 7 (**Si**) belonging to the broken Si−O bond. Their charge decrease constitutes 37% and 54% of the initial values, respectively. However, the most pronounced is the appearance of the equal-to-unity spin density at both atoms and the decrease of the summary WBIs by unity as well. Consequently, the free valency indices appear equal to unity at both atoms. As has been pointed out for the first time in ref 32, the free index appearance, which indicates a lifted chemical activity of the atoms involved, is ultimately connected with nonzero spin density. The latter is undoubtedly connected with nonpaired electrons that, in turn, is a conventional distinctive characteristic of a radical state. Therefore, the two last lines in Table 1 characterize the fragments of the Si4

molecule formed after a bond breaking as radicals. On the other hand, they cover the data, which as a whole can be regarded as a quantitative certificate specifying the radical state in general. According to the latter, any radical is characterized by lowering the charge of the atom involved by an absolute value, by an equal-to-unity spin density, and by a close-to-unity free valency index for the atom that is connected by excluding one of its electrons from the bonding with the other atoms.

Coming back to the discussion of the mechanochemical reaction occurring in PDMS oligomers when a bond of the backbone siloxane chain is broken, one can conclude that reaction equations (R1) and (R2) describe a homolytic mechanochemical reaction when radicals are the final products. This finding correlates with the radical character of organic polymers fracture that is well-known[2] as well as with a statement that in the majority of dielectric materials the fracture occurs as a result of a radical mechanochemical reaction.[33]

Dynamic Characteristics of the Deformation

The dynamic characteristics of the deformation performed involve a set of curves related to energy−elongation, force−elongation, and stress−strain interrelations. Figure 8 shows the first one presented as a dependence of the oligomer heat of formation on the MIC length. As seen from the figure, all three oligomers behave quite similarly. The energy−elongation curves exhibit two regions with remarkably different behavior. The first region is characterized by a practically unchanged energy, while the MIC length increases approximately twice with respect to the initial value. The second region starts with a close-to-parabola increase in the energy and a period of elastic deformation, which is followed by a clearly seen saturation in the energy inherent to the plastic deformation. A bond rupture that, in turn, is accompanied by an abrupt falling of the energy then accomplishes the latter.

The behavior is consistent with the structural transformation of the molecules discussed in details in section 2. The nearly constant-energy region is related to the deformation of the torsion and bond angles. The deformation occurring in the elastic region is connected with the elongation of the Si−O valence bonds.

Most pronouncedly the result discussed above is seen in Figure 9a, where force−elongation interrelations are presented. As previously, the dependence follows the same pattern for all three molecules and reveals two different regions. Being a derivative curve, the force−elongation dependence exhibits the nearly constant energy behavior discussed above in more detail. Actually, the energy constancy is maintained only on average. Discretely spread forces, small by value, accompany some changes in the molecular structure when the MIC is elongated. These very molecular configurations corresponding to the related peaks on the considered force−MIC-elongation curves are presented in Figures 2 and 3. It should be noted as well that the weak force appearance coincides with a small nonzero changing in the bond length in the MIC length range of 6−12 Å shown for the Si5 molecule in Figure 4.

The elastic region is presented by a linear dependence of the force from the MIC elongation. Approximating the intersection with the abscissa, the curves indicate reference MIC lengths, l_0, which correspond to the start of the linear dependence, depicting the beginning of the elastic deformation. The l_0 values thus determined will be used later when defining strain values in the region. The forces of response, corresponding to the elastic region, are shown in Figure 9b versus the strain of the MIC, ϵ, where $\epsilon = (L - l_0)/L$. The maximum of the triangle-like bands determines the calculated limit of the force of response, F_{max},

Deformation of Poly(dimethylsiloxane) Oligomers

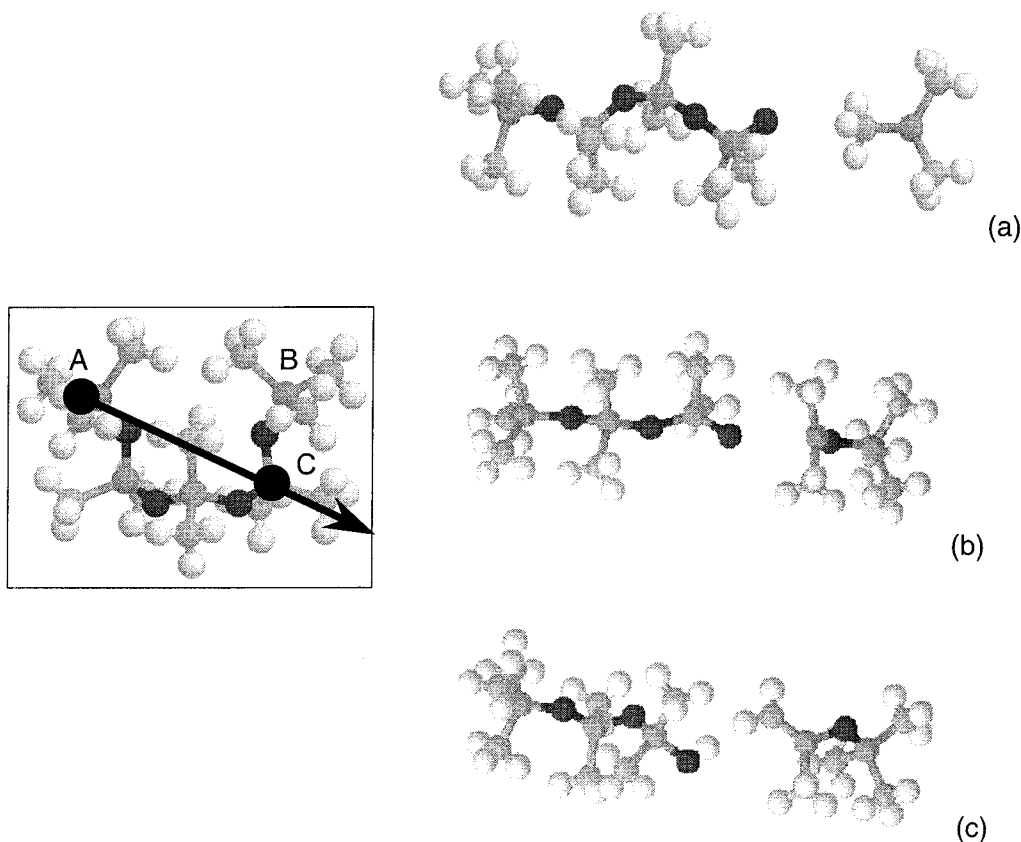*J. Phys. Chem. A, Vol. 103, No. 51, 1999* **11361**

(a)

(b)

(c)

Figure 7. Products of the mechanochemical reaction of a Si−O bond breaking. (a) Loading scheme see in Figure 1b. (b) Loading scheme is shown in the insert, the products formed just after the bond breaking. (c) The same as in (b), but after relaxation.

TABLE 1: Atomic Characteristics at a Si−O Bond Break (Si4 Molecule)[27]

NN	atom	charge	spin density	sum over Wiberg's coeff	free valency index
			Unloaded Molecule		
1	Si	0.64572	0	3.82118	0.17882
2	O	−0.54664	0	2.05719	−0.05719
3	Si	0.83811	0	3.72894	0.27106
4	O	−0.54791	0	2.06706	−0.06706
5	Si	0.83729	0	3.73185	0.26815
6	O	−0.54690	0	2.05832	−0.05832
7	Si	0.65205	0	3.81552	0.18448
			Molecule after Breaking		
1	Si	0.64739	0.00012	3.81862	0.18138
2	O	−0.53777	−0.00004	2.06212	−0.06212
3	Si	0.83361	0.00262	3.73258	0.26742
4	O	−0.54458	0.00736	2.07398	−0.07398
5	Si	0.83317	0.13955	3.72999	0.27001
6	**O***	**−0.34427**	**−0.97822**	**1.04708**	**0.95292**
7	**Si***	**0.29654**	**1.07241**	**2.98015**	**1.01985**

for the studied molecules. The area under these bands determines the work, A_{def}, needed for the elongation of all Si−O bonds and the breaking of one of them. The corresponding values of the limit force and the work are presented in Table 2. As seen from Figure 9 and Table 2, a tendency for the continuous decrease of the force is observed when the oligomer molecule size increases, while the corresponding work behaves oppositely.

In the practice of mechanical experiments, stress−strain interrelation is much more habitual. The corresponding curves for the considered molecules, whose starting points coincide with the beginning of the elastic deformation region, are depicted in Figure 10. The stress is determined as the response force shown in Figure 9b divided by the molecule's cross sectional area. The latter value for the oligomers is taken to be constant
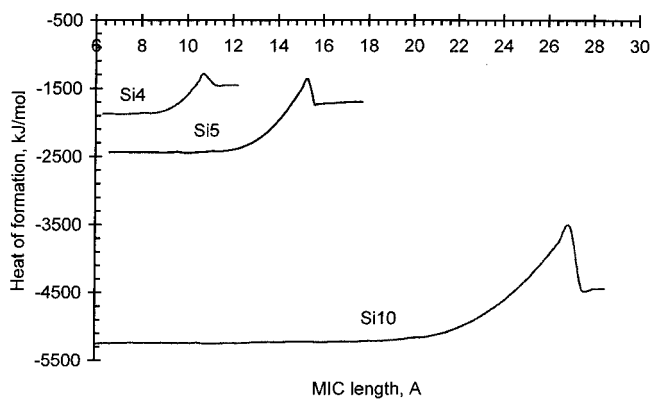

Figure 8. Heat of formation of the Si4, Si5, and Si10 molecules subjected to tensile deformation.

and equal to 1.182×10^5 m²/mol (the cross section is considered to be a circle of 5 Å in diameter). The maximum values of the stress, characterizing the strength of the related oligomer backbone, σ_{max}, are given in Table 2. As seen from the table, the calculated oligomer strength constitutes 50−35 GPa. Experimentally, the only data related to technical silicone rubber[34] give the value of ∼0.01 GPa that is less than the calculated one by 4 orders of magnitude. The reasons for such a drastic discrepancy will be discussed later.

Concluding, Figure 11 presents a general picture of the processes accompanying the PDMS oligomer deformation expressed via the dependence of the force of response versus a relative elongation of the MIC, L/L_0, where L_0 is the starting length value of the MIC. As seen in Figure 11a, the deformation starts and develops at the beginning as a rubber-like high-elasticity state, which is successively followed by elastic and plastic states. Then, the bond breaking occurs which introduces
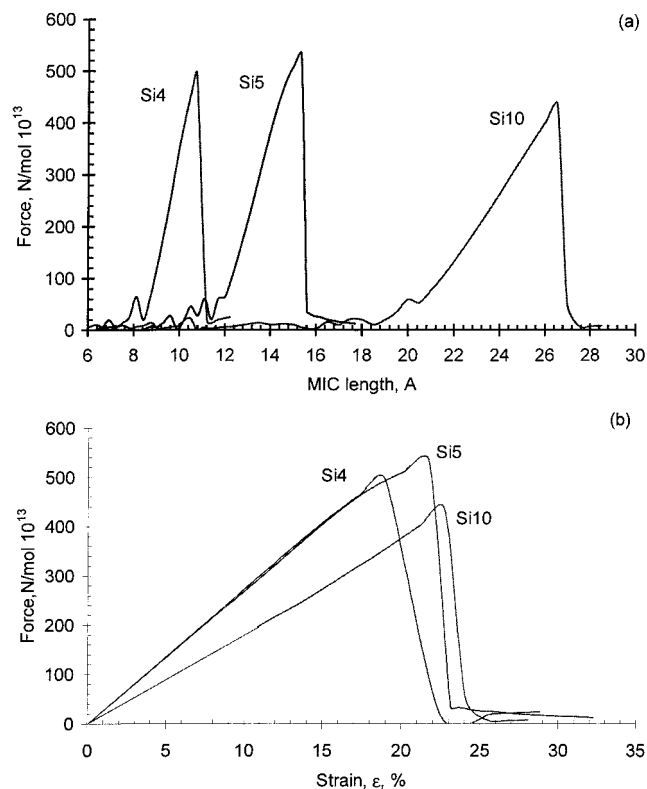
Figure 9. Force of response of the Si4, Si5, and Si10 molecules subjected to tensile deformation. (a) Total view. (b) Elastic region.
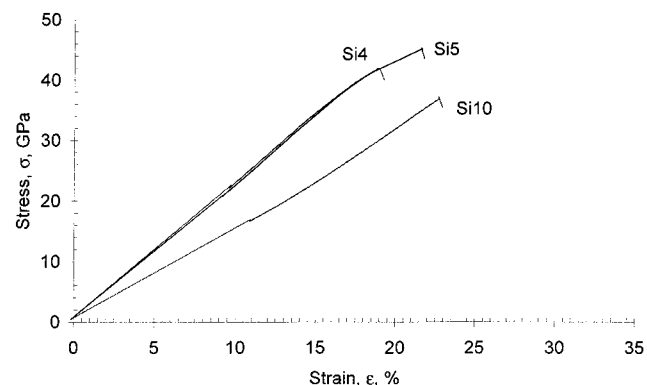

Figure 10. Stress−strain curves of the Si4, Si5, and Si10 molecules.

TABLE 2: Calculated Mechanical Characteristics for the PDMS Oligomers

oligomer	F_{max}, kJ/mol A	A_{def}, kJ/mol	σ_{max}, GPa	*E*, Gpa "w"	"σ"
Si4	495	894	42	296	230
Si5	533	1098	45	297	228
Si10	435	1473	37	213	157

the postbreaking state governed by the behavior of the formed radicals. Following from earlier statements, conformational changing of the molecule, which concerns the changes of the torsion and bond angles, causes the rubber-like state. Therefore, the high-elasticity behavior of the PDMS elastomers is actually connected with their high conformational ability, which was intuitively implied previously.[35] And this is the very point where silicone polymers differ from more rigid, say, organic counterparts. As for the elastic and plastic states, the elongation of chemical bonds determines those characteristics. In these regions, both silicone and organic polymers must behave quite similarly.
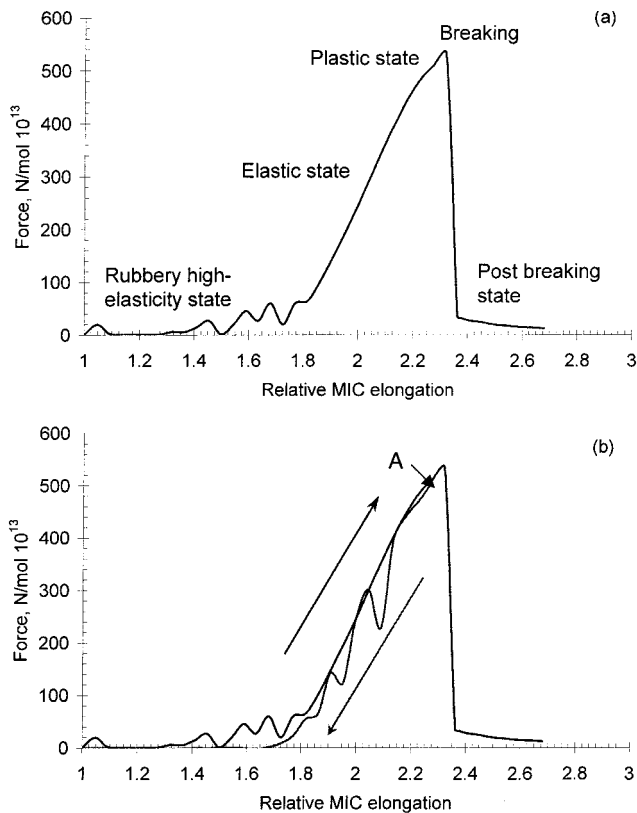

Figure 11. Generalized picture of the PDMS oligomer deformation. (a) Classification of the deformational process. (b) Force−strain hysteresis.

The high conformational ability of the PDMS oligomers dictates as well a peculiar behavior of the force-elongation hysteresis that is clearly seen in the elastic region. As shown in Figure 11b, a peculiarly oscillating curve is observed instead of a monotonic linear one when the MIC elongation is inverted at point A. The oscillations are evidently due to the conformational changing of the molecule structure, which creates this complicated hysteresis shape. The hysteresis is usually attributed to the internal friction in a loaded body.[36] As shown above, the conformational changes are responsible for the friction.

Young's Moduli of PDMS Oligomers

As is well-known from the dynamic theory,[2] in the harmonic approximation the energy of elastic deformation is expressed as

$$W(\epsilon) = {}^1/_2 v_0 E \epsilon^2 \qquad (8)$$

where ϵ depicts the strain, v_0 describes the molecular volume involved in the deformation, and *E* is the related Young's modulus. The energy $W(\epsilon)$ is determined, consequently, as the difference between two values of the heat of formation related to the current and reference values of the MIC,

$$W(\epsilon) = \Delta H(L) - \Delta H(l_0) \qquad (9)$$

Figure 12 shows $W(\epsilon)$ curves related to the studied molecules. When plotting, the reference l_0 values were taken as the corresponding points of intersection of the approximated linear dependencies of the force−elongation curves in Figure 9. As seen from the figure, the presented curves look actually like parabolic ones in a large region of ϵ that allows an approximation by exact parabolas by using the least-squares fitting to

Deformation of Poly(dimethylsiloxane) Oligomers

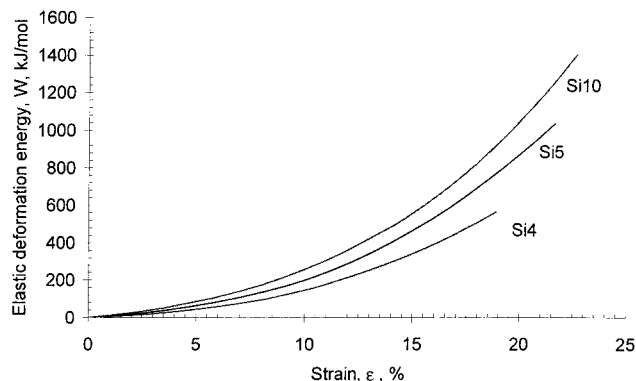*J. Phys. Chem. A, Vol. 103, No. 51, 1999* **11363**

Figure 12. Energy of the elastic deformation of the Si4, Si5, and Si10 molecules.

TABLE 3: Mechanical Characteristics of Organic Polymers

polymer		σ_{max}, GPa	E, Gpa
polyethylene	calcd[2]		316
	expt[36]	0.020	0.002
polyamide	calcd[2]		170
	expt[36]	0.160	3.500

determine the corresponding Young's moduli. Thus, obtained E values are listed in Table 2 and marked by a subscript "w". The molecular volume was determined therewith as $v_0 = S*l_0$, where S is the above-mentioned area of the molecule cross section of 1.182×10^5 m²/mol and l_0 is the MIC length at the start of the elastic region.

Besides the energy of the elastic deformation, stress−strain curves following the law of $\sigma = E\epsilon$ are another, more convenient source for the determination of Young's moduli. The related stress−strain curves are shown in Figure 10. As previously, when plotting, the above-described reference l_0 values were used to determine the coordinate origin. As seen from the figure, the curves are well approximated by straight lines in a large region of the ϵ values. The lines' slopes determine the Young's moduli directly. The values thus obtained and marked by a subscript "σ" are listed in Table 2. As seen from the table, the discrepancy between E_W and E_σ is about 30%, which is quite a coincidence in the values if one takes into account the difference in the approximation procedures applied. An experimentally known value for the Young's modulus of technical silicone rubber is 0.001 GPa,[34] which is less than the calculated one by about 5 orders of magnitude. The reasons for such behavior will be discussed in the next section.

**Mechanism of PDMS Polymer Fracture**

Data presented in Table 2 differ from the experimental values of both the oligomer strengths and Young's moduli by many orders of magnitude. The situation is fully analogous with that occurring for organic polymers.[2] Table 3 displays data on some technical species where a many-order discrepancy for the Young's moduli is evidently seen. On the other hand, when the Young modulus for, say, polyethylene, is measured for a monocrystalline whisker,[37] the difference between the calculated and measured values does not exceed 20%.[3,38] To explain this dramatic situation, Zhurkov et al. suggested a radical-driven mechanism for the organic polymer fracture[10] occurring in amorphous species. Schematically, the suggested mechanism is shown in Figure 13a. The deformation-induced scission of a C−C bond causes a formation of two radicals with a piloting methylene group for each. The pilot groups provoke the scission of two next C−C bonds belonging to neighboring chains, which is followed by the formation of two new methylene groups,

while the previous ones are terminated by the formation of two stable methyl and vinyl end groups. NMR and IR studies have revealed that the number of radicals and terminated groups differ by 3−4 orders of magnitude thus showing that a pair of radicals initiates the scission of 10^3−10^4 bonds.

Since C−C and Si−O bonds are quite similar from the dynamical viewpoint,[39] it seems to be reasonable to extend the above mechanism over PDMS polymers as well. As mentioned earlier, when a Si−O bond is broken, two radicals with piloting oxygen and silicon atoms are formed (see (R1)). When the first of them meets a neighboring siloxane chain,

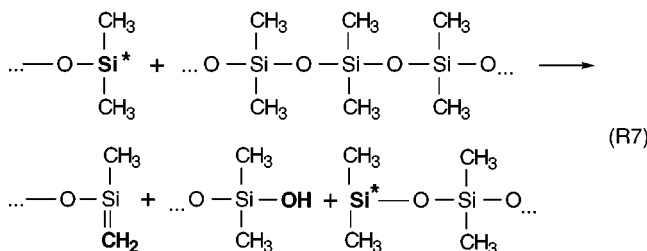$$\text{—O—Si—O}^* + \ ..\text{O—Si—O—Si—O—Si—O}.. \quad \text{(R4)}$$
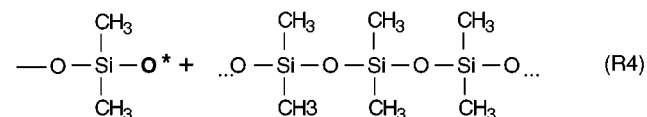
a stimulated passing of a hydrogen atom from the methyl group of the chain to the radical occurs so that the initiating radical is stabilized by the hydroxyl end group while a methylene radical is implanted in the chain body.

$$\text{—O—Si—OH} + \ ..\text{O—Si—O—Si—O—Si—O}.. \quad \text{(R5)}$$
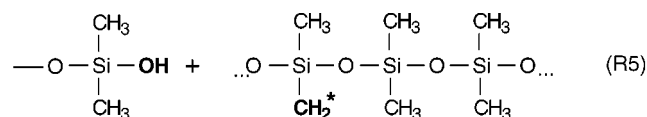
The radical provokes the break of a Si−O bond so that a stable molecular fragment with the methylene terminating end group is formed, while the other fragment is again an oxygen-piloting radical.

$$..\text{—O—Si—OH} + \ ..\text{O—Si} + \text{—O}^*\text{—Si—O—Si—O}.. \quad \text{(R6)}$$
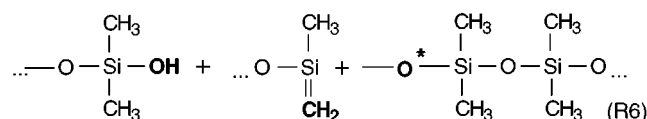
Similarly, the reaction piloted by a **Si***-headed radical looks like the following:

$$..\text{—O—Si}^* + \ ..\text{O—Si—O—Si—O—Si—O}.. \longrightarrow$$
$$..\text{—O—Si} + \ ..\text{O—Si—OH} + \text{Si}^*\text{—O—Si—O}.. \quad \text{(R7)}$$

and again two molecular fragments terminated by the methylene and hydroxyl end groups are formed, and a new **Si***-headed piloting radical is formed.

The suggested mechanism of the PDMS polymer fracture requires a convincing confirmation that can be done, in particular, by IR spectroscopy which can reliably fix the vibrations of the methylene and hydroxyl groups as in the case of the methyl and vinyl end groups of organic polymers.[2] At the same time, the suggestion throws light on a possible reason for the PDMS reinforcement by filling it with disperse silica. The matter is that any action preventing the spreading of the above fracture reaction will lead to the reinforcement. On the other hand, the reaction proceeds most favorably when there are conditions promoting conformational motions that stick the neighboring chains together for the reaction to proceed. Any full or partial immobilization of the polymers, such as crystal-
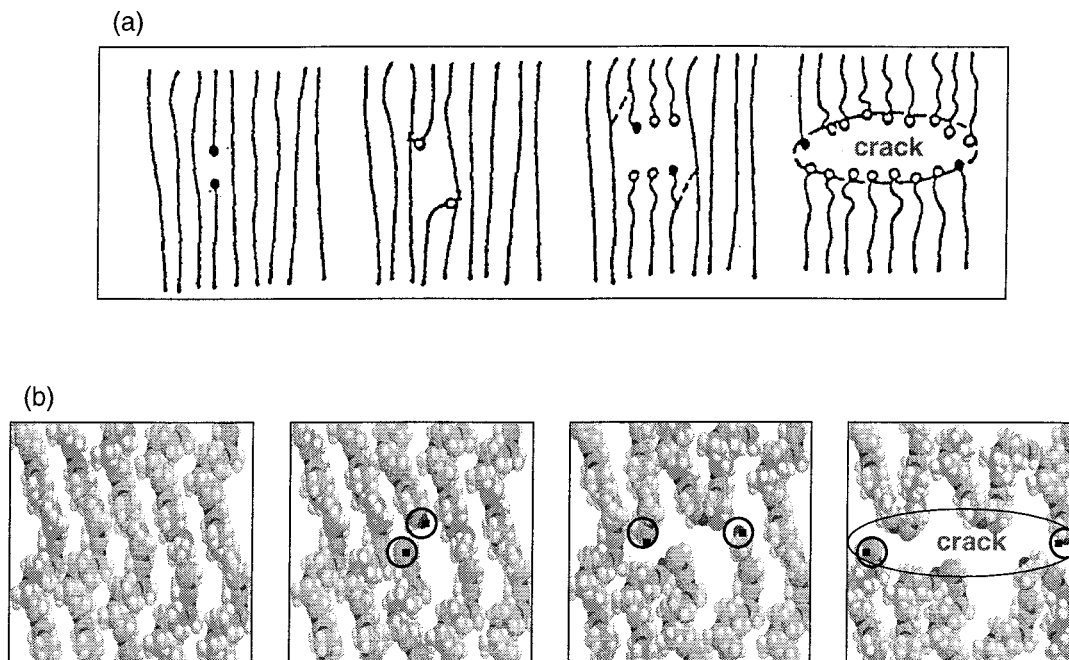
(a)

(b)

Figure 13. Scheme of the Zhurkovs et al. mechanism of polymer fracture. (a) Accepted for organic polymers.[2,10] (b) Suggested for silicone polymers.

lization or adsorption, will undoubtedly stop the reaction, which will result in strengthening the material.[40]

Conclusion

The paper presents results of a quantum mechanochemical study of a series of poly(dimethylsiloxane) oligomers subjected to uniaxial tension. The study is based on the introduction of a particularly specified mechanical internal coordinate (MIC) which describes the deformational mode. The calculations have been done following the coordinate-of-reaction concept performed in a total-energy minimization at every step of the constant-pitch elongation of the MIC. The residual total-energy gradient along the MIC is attributed to the force of response. The fact that the calculations were performed in internal coordinates has given a superior possibility to connect a physical deformation with intimate properties of the molecules studied.

Three linear PDMS oligomers Si4, Si5, and Si10 have been studied. An atomic reconstruction of their structures completed by a Si−O bond rupture has been traced at all stages of the deformation. A common behavior of all three species has been observed. Three stages of deformation differing by a structural transformation have been detected. As occurred, the conformational transformation in the molecular structure caused by changing either torsion (stage 1) or bond (stage 2) angles is responsible for the deformation resulting in about doubling of the initial MIC length. Both stages practically require no energy. The stages are followed by a chemical bond stretching (stage 3) resulting in a Si−O bond rupture due to a mechanically stimulated reaction. The main losses of the energy are connected with this stage.

The reaction products just formed have been analyzed from the electronic property viewpoint. As occurred, two noncharged molecular fragments headed by nonsaturated oxygen and silicon atoms have been produced whether an interior or an end Si−O bond is broken. The heading atoms possess an equal-to-unity spin density that convincingly points out their radical nature.

The observed structural deformational stages have been analyzed from the energetic viewpoint. Energy−strain, force−strain, and stress−strain interrelation have been studied. As

mentioned, the conformation-driven stages 1 and 2 are characterized by close to zero energetic parameters. Stage 3 caused by chemical bonds elongation involves elastic and plastic regions of deformation as well as the molecule breaking. Analyzing the energy−strain and stress−strain interrelations, the limiting values of the oligomer strength as well as their Young's moduli have been determined. A tendency to decrease in the values when the molecule size increases has been observed. It was shown that the conformation-driven stages of deformation are responsible for the high-elasticity or rubber-like state of the oligomers as well for the inner friction causing a peculiar stress−strain hysteresis.

Comparing the calculated and experimental data for the oligomer strength and Youngs' moduli, a many-order inconsistency has been exhibited similarly to that known for organic polymers. The finding has stimulated to suggest the Zhurkov's et al. radical-driven mechanism of the polymer fracture, accepted for organic species, to be extended for silicone species as well. The mechanism throws light into the reinforcement of the latter by filling them with highly disperse silica. The polymer immobilization caused by adsorption might stop the fracture reaction, thus reinforcing the material.

References and Notes

(1) Mark, J. E.; Erman, B. *Rubberlike elasticity*; Wiley: New York, 1988.

(2) Tashiro, K. *Prog. Polym. Sci.* **1993**, *18*, 377.

(3) Klei, H. E.; Stewart, J. P. *Int. J. Quantum Chem. Symp.* **1986**, *230*, 529.

(4) Wierschke, S. G. *Mater. Res. Soc. Symp. Proc.* **1989**, *134*, 313.

(5) Bordeaux, D. S. *J. Polym. Sci., Polym. Phys. Ed.* **1973**, *11*, 1285.

(6) Yushchenko, V. S.; Ponomareva, T. P.; Shchukin, E. D. *J. Mater. Sci.* **1992**, *27*, 1659.

(7) Yushchenko, V. S.; Shchukin, E. D.; Hotokka, M. *J. Mater. Sci.* **1993**, *28*, 920.

(8) Khavryutchenko, V.; Nikitina, E.; Malkin, A.; Sheka, E. *Phys. Low-Dimens. Struct.* **1995**, *6*, 65.

(9) Khavryutchenko, V. D.; Khavryutchenko, A. V., Jr. *DYQUAMECH*, Dynamical-Quantum Modelling in Mechanochemistry Software for Personal Computers; Institute of Surface Chemistry, National Academy of Science of Ukraine: Kiev, 1993.

(10) Zhurkov, S. N.; Vettegren, V. I.; Korsukov V. E.; Novak I. I. *Fracture* **1965**, 545.

Deformation of Poly(dimethylsiloxane) Oligomers

J. Phys. Chem. A, Vol. 103, No. 51, 1999 **11365**

(11) Kuzminski, A. S.; Sedov, V. V. *Khimicheskie prevrashchenia elastomerov (Chemical Transformations of Elastomers)*; Khimia: Moskwa, 1984.

(12) Pluvinage, G. *Machanique Elastoplastique de la Rupture*; Cepad: Tuluse, 1989.

(13) Bartenev, G. M. *Prochnost i mekhanizm razrushenia polimerov (Strength and Destruction Mechanism of Polymers)*; Khimia: Moskwa, 1984.

(14) Stepanov, V. A.; Peschanskaya, N. N.; Shpeyzman, V. V. *Prochnost i relaksacionnye javlenia v tverdykh telakh (Strength and Relaxation Phenomena in Solids)*; Nauka: Leningrad, 1984.

(15) Gutman E. M. *Mekhanokhimia metallov i zashchita ot korrosii (Mechanochemisrty of Metals and Protection from Corrosion)*; Metallurgia: Moskwa, 1974.

(16) Baranbojm, N. K. *Mekhanokhimia vysokomolkulyarnykh soedinenij (Mechanochemistry of High-Molecular Compounds)*; Khimia: Moskwa, 1978.

(17) Avvakumov, E. G. *Mekhanicheskie metody aktivacii khimicheskich processov (Mechanical Ways for Chemical Process Activation)*; Nauka: Novosibirsk, 1979.

(18) Tobolski, A.; Eyring, H. *J. Chem. Phys.* **1943**, *11*, 125.

(19) Dewar, M. J. S. *Fortschr. Chem. Forsch.* **1971**, *23*, 1.

(20) Khavryutchenko, V. D.; Khavryutchenko, A. V., Jr. *DYQUAMOD*, Dynamical-Quantum Modelling Software for Personal Computers; Joint Institute for Nuclear Researchs, Dubna and Institute of Surface Chemistry: National Academy of Science of Ukraine: Kiev, 1993.

(21) Sheka, E. F.; Khavryutchenko, V. D.; Nikitina, E. A. *Phys. Low-Dimens. Struct.* **1995**, *1*, 1.

(22) Ignatjev, I. S.; Tenisheva, T. F. *Kolebatelnye spectry i elektronnoje stroenie molekul s uglerod-kislorodnymi i kremnij-kislorodnymi svyasyami (Vibrational Spectra and Electronic Structure of Molcules with C−O and Si−O bonds)*; Nauka: Leningrad, 1991.

(23) Pulay, P. *Theor. Chim. Acta* **1979**, *50*, 299.

(24) Clark, T. *A Handbook of Computational Chemistry. A Practical Guide to Chemical Structure and Energy Calculations*; Wiley-Interscience: New York, 1985.

(25) Stewart, J. P. *J. Comput. Chem.* **1989**, *10*, 209, 221.

(26) The molecular force field has been obtained quantum chemically and then corrected in the course of the inverse spectral problem solution to fit precisely the experimental vibrational spectra of the molecule recorded by IR transmission and inelastic neutron scattering: Sheka, E. F.; Khavryutchenko, V. D.; Nikitina, E. A.; Natkaniec, I.; Barthel, H.; Weiss, J. *Proceedings of the German-Russian Users Meeting, Condense Matter Physics with Neutrons at IBR-2*; Frank Laboratory of Neutron Physics, JINR: Dubna, 1998; p 122.

(27) Since the bond breaking disjoins electrons of atoms involved in the bond, a question arises of whether the closed-shell approximation used throughout the paper is valid for the bond rupture description. As shown in the current study, the approximation correctly describes space structure and heat of formation of the molecule under deformation at every step, including the bond rupture. However, at the very point of the bond breaking, it fails in describing the quantities related to the electron density matrix since it does not distinguish α and β spins. This makes difficult a proper characterization of final products of the reaction. To remove the difficulty, the values given in Table 1 were obtained in the open-shell approximation of the PM3 technique (for reference, see: *HyperChem. Computational Chemistry*; Hypercube, Inc.: Waterloo, 1994; Part 2). As in the case of the closed-shell one, a spin-singlet configuration of the molecular electronic state was considered only.

(28) Semenov, S. G. In *Razvitije uchenia o valentnosti (Evolution of the Valency Doctrine)*; Khimia: Moskva, 1977; p 117.

(29) Wiberg, K. B. *Tetrahedron* **1968**, *24*, 1083.

(30) Khavryutchenko, V.; Sheka, E.; Aono, M.; Huang, D. H. *Phys. Low-Dimens. Struct.* **1996** *11/12*, 1.

(31) Coulson, C. A. *Valence*, 2nd ed.; Oxford University Press: New York, 1961.

(32) Khavryutchenko, V.; Sheka, E.; Aono, M.; Huang, D. H. *Phys. Low-Dimens. Struct.* **1998**, *3/4*, 81.

(33) Berstein, V. A. *Mechanogidroliticheskie processy i prochnost tverdykh tel (Mechanohydrolitic Processes and Strength of Solids)*; Nauka: Leningrad, 1987.

(34) Data obtained at Wacker Chemie GmbH.

(35) Sometimes, the rubber-like high elasticity is presented as an entropy-driven process while the elastic and plastic regions are connected with changes in enthalpy. This picture correlates well with the vibration-dynamical presentation discussed in section 2. Actually, the entropy is the most essential when the related enthalpy is small. These conditions are met at Stages 1 and 2 of the deformational process considered. As is known (Dewar, M. J. S.; Ford, G. *J. Am. Chem. Soc.* **1977**, *99*, 7822), the most valuable contribution to the entropy of a molecular system is provided by the lowest frequency vibrations, which are presented by torsions and bendings in the studied case.

(36) *Enziklopedia polimerov (Polymer Enciclopedia)*; Sovetskaja enciklopedia: Moskwa, 1974; t.2, p 230.

(37) Tashiro, K.; Kobayashi, M. *Polymer* **1991**, *32*, 454.

(38) The many-order difference in the strength of crystalline and amorphous polymers is widely known.[1]

(39) The related frequencies of the stretching vibrations fill in the range of 1000−1200 and 800−1000 cm^{-1} for the C−C and Si−O bonds, respectively. The ratio of squared frequencies, which determines the ratio of the corresponding Young's moduli, ranges between 1.5 and 2.5. As seen from Tables 2 and 3, the calculated *E* values provide the ratios falling into the interval of 1.5−2.74, which is perfectly consistent with the above-mentioned data.

(40) It should be taken into account as well that, unlike the majority of organic polymers, silicone polymers are cross-linked, which may provide additional ways for the polymers to be strengthened.